JOURNAL OF SPACECRAFT AND ROCKETS
Vol. 48, No. 4, July–August 2011

Application of System-Identification Techniques to Health Monitoring of On-Orbit Satellite Boom Structures

Yingtao Liu,* Seung Bum Kim,† and Aditi Chattopadhyay‡
Arizona State University, Tempe, Arizona 85287
and
Derek Doyle§
U.S. Air Force Research Laboratory, Kirtland Air Force Base, New Mexico 87117

DOI: 10.2514/1.51818

The integration of composites into spacecraft is challenged by the risk of damage initiation and propagation during storage, launch, and service life. Elastically deployable composite booms are being developed for space utility. Matrix cracks are considered a primary form of damage caused by packaging before launch. However, while on orbit, most damages are induced by the environmental effects on the polymers. A well-developed structural health monitoring system will provide information for the dynamic control of the satellite and the condition of the deployable mechanisms on the space vehicle. A structural health monitoring methodology, based on the system-identification techniques, is proposed to identify the structural degradation in laminated composite booms. Nondestructive evaluation techniques, frequency-response analysis and autoregressive with exogenous input models are used to approximate the transfer functions between input and output sensing signals. Structural degradation is identified by examining the change of transfer functions at different storage states. A single-input/single-output approach is adopted in this paper. The proposed methodology is validated through experimentation in which matrix cracking is gradually induced by packaging the sample.

Nomenclature

a	=	output parameters of the autoregressive with exogenous input model
b	=	input parameters of the autoregressive with exogenous input model
DI	=	damage index
G	=	frequency-response function
R	=	amplitude ratio of frequency-response function
R^N	=	recorded input/output measurement
S	=	spectral densities, W/Hz
s	=	storage state
x	=	input signal
y	=	output signal
δ	=	angle of phase shift, deg
ε	=	estimation error of autoregressive with exogenous input model
θ	=	adjustable parameters in the vector form
τ	=	time delay, s
ϕ	=	phase of frequency-response function
φ	=	previous input/output measurement
ω	=	signal frequency, Hz

Presented as Paper 2010-3027 at the 51st AIAA/ASME/ASCE/AHS/ASC, Structures, Structural Dynamics, and Materials Conference, Orlando, FL, 12–15 April 2010; received 29 July 2010; revision received 29 March 2011; accepted for publication 30 March 2011.

*Graduate Research Associate, School for Engineering of Matter, Transport and Energy. Student Member AIAA.
†Postdoctoral Research Associate, School for Engineering of Matter, Transport and Energy.
‡Professor, School for Engineering of Matter, Transport and Energy. Fellow AIAA.
§Symbiotic Structures Lead, Space Vehicles Directorate, 3550 Aberdeen Avenue SE. Professional Member AIAA.

I. Introduction

ADVANCED carbon/epoxy composites have been widely used for a variety of structural components in spacecraft, due to their light weight, dimensional stability, and optimized mechanical properties [1]. On-orbit satellite systems operate in a harsh environment and the structural degradation of composite components can be caused by various sources such as atomic oxygen, ultraviolet (UV) radiation, proton and electron radiation, vacuum, and thermal cycling [2–4]. Although the coefficient of the thermal expansion (CTE) of composites is commonly near zero and significantly less than typical aluminum, composites are just as vulnerable to the environmental influences. High vacuum pressure can lead to material outgassing, UV radiation can deteriorate the surface matrix and discolor the surface, changing the thermal performance, and debris can shatter supports, as was the case for the Cerise microsatellite that had a catalogued item severed and locally vaporized by impact on its Earth-pointing boom [5]. Like most space mishaps, the system was recoverable, but difficult to diagnose.

Damage in composite satellite structures, such as matrix cracks and matrix-fiber debonding, causes the degradation of structural stiffness and can affect the dynamic response of the satellite system during maneuvers such as slewing or deployments. Structural degradation needs to be monitored to update the dynamic control system of the spacecraft. Developing a structural health monitoring (SHM) system for monitoring the flexible structures of a satellite, such as the composite booms, will allow the satellite guidance, navigation, and control systems to incorporate any quantified stiffness degradation values into future functions. A properly designed SHM system will be able to detect, classify, and localize damage and determine if the composite components of the satellite will continue to perform safely and sufficiently. Price et al. [6] developed an integrated health monitoring system for real-time sensing of impact damages in aerospace vehicles using piezoelectric polyvinylidene fluoride transducer-based passive sensing and a self-organizing approach. Prosser et al. [7] compared a variety of sensor types, such as fiber optic sensors, carbon nanotube sensors, and acoustic emission sensors, and reported the data processing techniques for the sensor placement optimization and the damage identification of composite components in space vehicles. Zagrai et al. [8] detected and located loose bolts in complex space structures with a large number of bolted

joints using the embedded ultrasonic acoustic–elastic method, and the integrity of the bolted joint was evaluated by the stress-induced phase shift in the recorded elastic wave signals. Liu et al. [9] developed a condition-based SHM and prognosis methodology for composite structures under complex loading conditions. However, few on-orbit influences are considered in the previous literature. A SHM system for on-orbit composite components needs to be used not only to determine the status of a satellite structure before launch, but also for the on-orbit detection of damage. This can be seen in the case of the deployable antenna of the Mars Advanced Radar for Subsurface and Ionosphere Sounding (MARSIS) project on Mars express. The deployable antenna was made with glass fibers and collapsed in a manner to deploy using stored elastic energy. When it was time to deploy on orbit, the risk was considered unacceptable and it was never released, due to the concerns of deployment and how guidance and other functioning instrumentation would be impacted, along with the inability to diagnose any conditions after deployment [5].

Although significant research on SHM of composites has been reported in the last decade, most of the published work focuses on the macroscale damage, such as delamination and impact damage. Well-developed SHM techniques, including acoustic emission methods, have also shown to be effective in detecting macroscale damage in composites. However, the dominant structural degradation mode induced into a flexible composite boom before launching is matrix cracking. As shown in Fig. 1, the carbon-fiber-reinforced plastics boom in the stowed configuration and the fully deployed solar sail is developed by the DLR, German Aerospace Center. Both the CFRP booms and solar sail membranes are used as critical structural components of the propulsion system for the synthetic aperture radar satellites. When the solar sail membranes and CFRP boom are packed into a small volume, matrix cracking is introduced to the boom structure, due to the flattening and wrapping procedure. The detection of matrix cracking in composites requires more sensitive and reliable techniques. However, research in monitoring micro matrix cracks in composites is still in its infancy. In addition, most current nondestructive evaluation techniques, such as x-ray, ultrasonic scan, and radiography, are costly, time-consuming, labor-intensive and do not satisfy the responsive ground-based or on-orbit service. D'Amato et al. [12] used a global method for analyzing an unknown input signal through sensor-only noncausal blind identification. In that effort, which examined the same structure used in this paper, the sensing was done on the deployment mechanism, rather than on the boom, in order to reduce the complexity of eventual SHM integration. The integrity of the boom was then inferred from the accelerometer data on the rotating hub and analyzed as a psuedo frequency response. However, through reducing the complexity, the sensitivity of the system to adequately account for any level of stiffness loss was decreased. To compensate for this problem, researchers implemented adaptive model refinement using retrospective cost optimization. This provided significantly better insight into the degradation of the system. However, when inferring structural integrity of a component through analysis of a different component, there must be the assumption that there are no other changes in the system chain between both elements that may result in a false analysis of the state of the booms. A SHM system that automatically monitors and detects on-orbit degradation of composite components is required for the reliable use of composite satellite structures.

System-identification techniques have been used for structural evaluation of both metallic and composite structures to interpret data and extract diagnostic features. The extraction of damage-sensitive features from experimental measurements or simulation, and the statistical analysis of these features determine the current state of the system's health. Nonparametric models (such as frequency-response methods) and parametric models (such as state-space models) are the two main approaches for system-identification techniques. Park et al. [13] used an inverse method for identifying the damage location and the impact force–time history on composite plates using the state-space estimation techniques. The transfer function at any point was constructed by interpolating four neighboring known transfer functions. However, the actual damage induced in the composite samples by the impact loading was not clarified. Different types of structural damage, such as fiber breakage and delamination, can be introduced by different impact velocities and energies. The nature of impact damage introduced into their composite specimens needs to be demonstrated, and the method also needs to prove functionality on complicated structures. Sohn et al. [14] presented a damage feature extraction approach by combining the autoregressive and auto-regressive with exogenous input (ARX) models and applied the two techniques to fiber optic strain-gauge data obtained from two different structural conditions of a surface-effect fast patrol boat. Although the damage features were identified by combining the two models, the procedure needs to be examined with composite structures and under more operational conditions before it can be applied as a SHM system for composite components. Mohanty et al. [15] proposed an unsupervised system-identification-based techniques to estimate the time-series fatigue damage states for metallic materials. To estimate the nonparametric damage state, ultrasonic broadband active sensing and correlation analysis were used. In most cases, the system-identification techniques showed acceptable performance for visible damage, such as cracks in metal and delamination in composites.

In this paper, a system-identification-based SHM technique is proposed to quantify the structural degradation of the composite booms used in satellite applications, as shown in Fig. 2. Low-frequency broadband sweep excitations are applied to the modeled samples using macrofiber composite (MFC) transducers. Structural degradation and changes in dynamic response of the samples are determined from the frequency response of measured actuator and sensor signals. The transfer functions of single-input/single-output (SISO) approach are estimated using the ARX model to identify the damage levels. A damage index is defined to describe the structural degradation condition in the booms. Both local and global structural

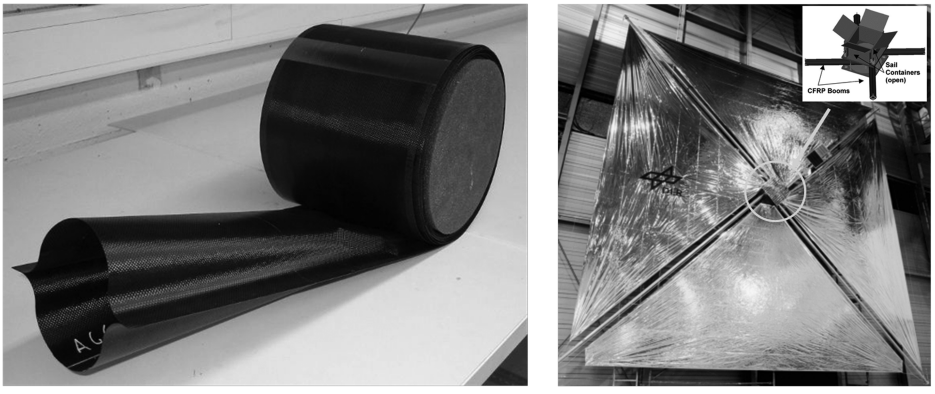

a) b)

Fig. 1 Photographs of a) the deployable DLR CFRP boom and b) solar sail [10,11].

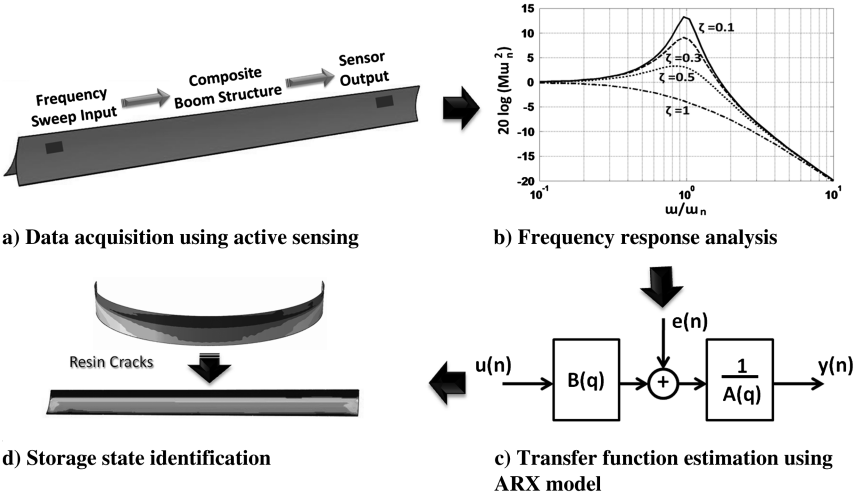

a) Data acquisition using active sensing

b) Frequency response analysis

d) Storage state identification

c) Transfer function estimation using ARX model

Fig. 2 SHM of composite booms based on a system-identification approach.

degradation estimations are completed by using the MFC data collected from different positions. The proposed method has been validated experimentally.

II. Structure Health Monitoring Framework for a Satellite Structure

A. Frequency-Response Method for System Identification

The frequency-response method for system identification characterizes the response of the composite boom subject to a sweep excitation. The frequency response is estimated using spectral analysis and can be expressed in a cross-correlation function and autocorrelation function. For time-domain input signal $x(t)$ and output signal $y(t)$, the spectral densities $S_{yx}(j\varpi)$ and $S_{xx}(j\varpi)$ of the relevant measured input and output are written as [16]

$$S_{yx}(j\varpi) = \tilde{y}(j\varpi)\tilde{x}^*(j\varpi) \tag{1}$$

$$S_{xx}(j\varpi) = \tilde{x}(j\varpi)\tilde{x}^*(j\varpi) \tag{2}$$

where $\tilde{x}(j\varpi)$ and $\tilde{y}(j\varpi)$ are the finite Fourier transforms of the relevant measured input and output, and $\tilde{x}^*(j\varpi)$ is the conjugate of$\tilde{x}(j\varpi)$.

By applying the finite Fourier transform to measured input and output data, an estimate of the frequency-response function can be written as

$$G(j\varpi) = \frac{S_{yx}(j\varpi)}{S_{xx}(j\varpi)} = \frac{\tilde{y}(j\varpi)\tilde{x}^*(j\varpi)}{\tilde{x}(j\varpi)\tilde{x}^*(j\varpi)} \tag{3}$$

where the frequency-response function, $G(j\varpi)$, is a complex vector. Both input/output magnitude ratio and phase shift are considered. The magnitude ratio $R(\varpi)$ and phase $\phi(\varpi)$ can be expressed as

$$R(\varpi) = \sqrt{\{\mathrm{Re}[G(j\varpi)]\}^2 + \{\mathrm{Im}[G(j\varpi)]\}^2} \tag{4}$$

$$\phi(\varpi) = \tan^{-1}\left\{\frac{\mathrm{Im}[G(j\varpi)]}{\mathrm{Re}[G(j\varpi)]}\right\} \tag{5}$$

The frequency-response method constitutes a describing function that linearly characterizes the behavior of the input-to-output MFC transducers. If the transfer function of the entire structure changes due to the induced matrix cracking, the Bode plot of input/output sensor measurements will provide guidance for the future construction of a system transfer-function model. Further details are explained later in the paper.

B. Transfer-Function Estimation Using the ARX Model

In this study, an ARX model is used to estimate the transfer function of the composite active sensing system. Traditional autoregressive and autoregressive moving-average models are fitted to the sensing signals (output signals) and do not consider the excitation signals (input signals). The ARX model considers the excitation signals as additional information in a time-series model. The input/output model can be reasonably estimated using the ARX model and the linear least-squares method [17,18]. As a typical example of the black-box model, the model is widely used, due to its simplicity. Ignoring the estimation error, the ARX model that describes the relationship between input $x(t)$ and output $y(t)$ is shown in Eq. (6) [19]:

$$y(t) + a_1 y(t-1) + \cdots + a_n y(t-n) = b_1 x(t-1) + \cdots + b_m x(t-m) \tag{6}$$

where a_i and b_j are the parameters of the ARX model, n is the number of poles, and m is the number of zeros. Once m and n are calculated, the ARX can be written as the ARX (m, n) model. The model assumes that the sampling interval is uniform in the time domain. To determine the next output value given by previous observation, it is easier to write Eq. (6) as

$$y(t) = -a_1 y(t-1) - \cdots - a_n y(t-n) + b_1 x(t-1) + \cdots + b_m x(t-m) \tag{7}$$

The parameters of the ARX model, a_i and b_j, are calculated from the sensor measurements $x(t)$ and $y(t)$ using the linear least-squares method. For a more compact notation, these adjustable parameters can be written in a vector form:

$$\theta = [\, a_1, \ldots, a_n \quad b_1, \ldots, b_m \,]^T \tag{8}$$

and the previous input/output measurement can be written as

$$\varphi = [\, -y(t-1), \ldots, -y(t-n) \quad x(t-1), \ldots, x(t-m) \,]^T \tag{9}$$

According to Eq. (9), the output estimation of the ARX model is

$$y(t) = \varphi^T(t)\theta \tag{10}$$

Note that the calculation of the next output measurement from previous data in vector φ depends on all the parameters in vector θ. The calculated value $\hat{y}(t|\theta)$ is different from the real measurement $y(t)$:

$$\hat{y}(t|\theta) = \varphi^T(t|\theta)\theta \tag{11}$$

All the unknown parameters in vector θ are calculated using the least-squares method. From the recorded input/output measurement

R^N, the unknown parameters can be calculated by minimizing the error $E(\theta, R^N)$ between the real output measurement $y(t)$ and the calculated output $\hat{y}(t|\theta)$. Here,

$$R^N = [x(1), y(1) \quad \cdots \quad x(N), y(N)] \tag{12}$$

$$E(\theta, R^N) = \frac{1}{N}\sum_{i=1}^{N}(y(t) - \hat{y}(t|\theta))^2 = \frac{1}{N}\sum_{i=1}^{N}(y(t) - \varphi^T(t|\theta)\theta)^2 \tag{13}$$

Set the derivative of $E(\theta, R^N)$ to zero,

$$\frac{\mathrm{d}}{\mathrm{d}\theta}E(\theta, R^N) = \frac{2}{N}\sum_{i=1}^{N}\varphi(t)(y(t) - \varphi^T(t|\theta)\theta) = 0 \tag{14}$$

resulting in

$$\sum_{i=1}^{N}\varphi(t)y(t) = \sum_{i=1}^{N}\varphi(t)\varphi^T(t|\theta)\theta \tag{15}$$

Because $\varphi(t)$ has been defined by the previous input/output measurement, all the parameters for the ARX model can be calculated using Eq. (16):

$$\theta = \left[\sum_{i=1}^{N}\varphi(t)\varphi^T(t|\theta)\right]^{-1}\sum_{i=1}^{N}\varphi(t)y(t) \tag{16}$$

The goal of system identification is to obtain a transfer function that predicts the output using input of the system reliably. From a given set of experimental data, the modeled data $\hat{y}(t|\theta)$ are compared with the experimental data $y(t)$ to minimize the error between the two data sets. Once θ is calculated, the transfer function can be obtained from Eq. (10).

C. Structural Degradation Identification Using the Damage Index

The accuracy and sensitivity of the defined damage index is critical for identifying matrix cracks in composites. Ideally, a composite structure without damage can be modeled as a linear system. However, composite structures present more nonlinear properties when nonvisible damages, such as matrix cracks, are introduced [20–22]. Although the ARX model can be expressed as shown in Eq. (6), an error term $\varepsilon(t)$ should be introduced to this model for the reconstruction accuracy. The modified ARX model can be expressed as

$$y(t) + a_1 y(t-1) + \cdots + a_n y(t-n) = b_1 x(t-1) + \cdots + b_m x(t-m) + \varepsilon(t) \tag{17}$$

It is assumed that the error between the measurement and estimation obtained by the ARX model is caused mainly by the nonlinear properties of matrix cracking in composites. The measurement noise is assumed to be uncorrelated with the input signal and can be ignored. The estimation error becomes larger when more nonlinearities due to matrix cracks are introduced. A clear definition of estimation error ε_s at storage state s is expressed as

$$\varepsilon_s = y_s(t) + \sum_{i=1}^{n} a_{i,s} y_s(t-i) - \sum_{j=1}^{m} b_{j,s} x_s(t-j) \tag{18}$$

where $a_{i,s}$ and $b_{j,s}$ are the parameters of the ARX model at storage state s, $y_s(t-i)$ $(i = 0, 1, \ldots, n)$ are the sensor output measurements at storage state s, and $x_s(t-j)$ $(j = 1, 2, \ldots, m)$ are the sensor input measurements at storage state s. The order of the ARX model is chosen by balancing the calculation error and cost. Once the order of the ARX model is chosen, a damage index can be defined as

$$\mathrm{DI}_s = \sqrt{\frac{[\varepsilon_s - \varepsilon_0]^2}{\varepsilon_0^2}} \tag{19}$$

where ε_0 is the estimation error for the referred initial storage level. When the healthy state of the structures is known, ε_s is the sth storage state with respect to the healthy state ($s = 0$). However, when the healthy state is unknown, the defined damage index DI_s can still be used to compare the later storage state with the reference storage level (the first available storage state).

III. Experimental Tests

To validate the system-identification-based SHM framework, a flattening and wrapping experiment was performed on composite booms, which were supplied by the U.S. Air Force Research Laboratory, Space Vehicles Directorate. The materials used for the composite booms are CFRP in unidirectional tape and plain-weave-fabric forms, both using Hexcel® IM7 fibers and M72 resin. The boom is composed of two flanges. The cross section of the boom is shown in Fig. 3. The stacking sequence of each flange is

$$[0°\text{tape}/0°\text{tape}/\pm 45°\text{weave}/0°\text{tape}/0°\text{tape}]$$

(0° is the long axis of the boom). These two laminates overlap at the ridge to form a $[0°/0°/\pm 45°/0°/0°]_s$ stacking sequence. The boom specimen was instrumented with four MFC transducers (Smart Material Corp., model M 2814 P1), as shown in Fig. 4. To obtain proper bonding conditions between the boom and the sensors, the sample surface was prepared with abrasive paper and cleaned with a cotton-tipped applicator. Stewart-MacDonald super glue (model 20-X) was used as the adhesive. The outgassing properties of this particular adhesive are not critical at the stage of research, but consideration should be addressed when applied to systems containing optical payloads where outgassing is a concern.

The primary source of degradation to the boom structure occurs during the flattening and wrapping process of the boom around a hub that is used to store the boom before deployment. The extent of matrix cracking and structural degradation due to flattening and wrapping the boom around the hub can be critical in the system response. As the stiffness changes due to matrix cracking, the system's response will be affected. The structural degradation incurred by storing the structure has been simulated experimentally using a wrapping fixture, as shown in Fig. 5. The wrapping fixture consists of a 14.-in.-diam hub around which the boom sample is wound. This fixture was constructed to test 24 in. samples. The boom was clamped, as shown in Fig. 5a with a 2.-in.-long clamping surface, flattening the clamped end of the boom to the hub. The boom was then wrapped taut around the center hub and clamped at the preset location. The rate of wrapping was approximately 1 in./s, which was necessary to ensure that the boom flattened properly and to maintain as little gap as possible from the center hub. Similar wrapping and deploying rates were used by the CFRP boom and solar sail

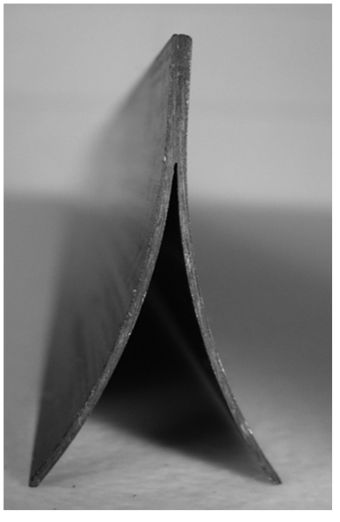

Fig. 3 Cross section of the AFRL composite boom.

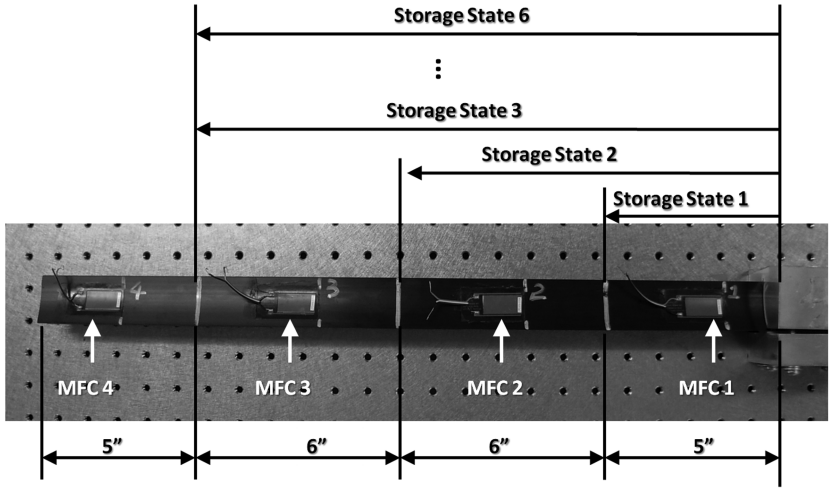

Fig. 4 Composite-boom specimen.

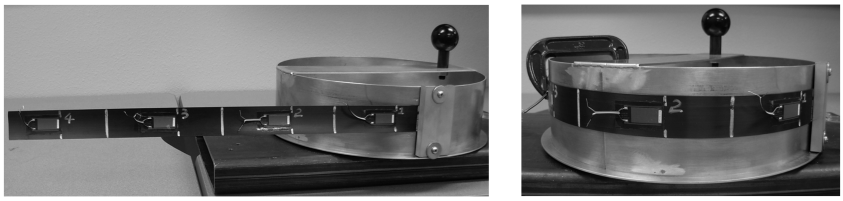

a) **b)**

Fig. 5 Composite boom in the wrapping machine at a) initial position of the composite and b) final wrapped position.

membrane of the synthetic aperture radar satellites developed by DLR [12].

The experimental procedure is shown in Fig. 6. Two substeps were completed before a new storage state was generated. MFC active sensing data were collected first. One MFC was used as the actuator to excite the boom specimen and the response was captured by the other three MFC transducers using a low-frequency sweep signal. The boundary condition of the boom specimen was traction-free. Modal analysis was conducted experimentally using a scanning-head laser vibrometer (Polytec, Inc., model VCS-310) and a vibration shaker (model VTS 100). The storage states were generated six times by flattening and wrapping the boom specimens to different arc lengths, as shown in Fig. 7. Storage state 1 was wrapping the specimen around the hub to introduce matrix cracks up to the section indicated (arc length of 5 in.). The boom specimen was clamped at the preset location for 30 s before being deployed to its initial position. In the second storage state, both sections 1 and 2 were used (arc length of 11 in.), and in storage states 3 to 6, sections 1–3 were all

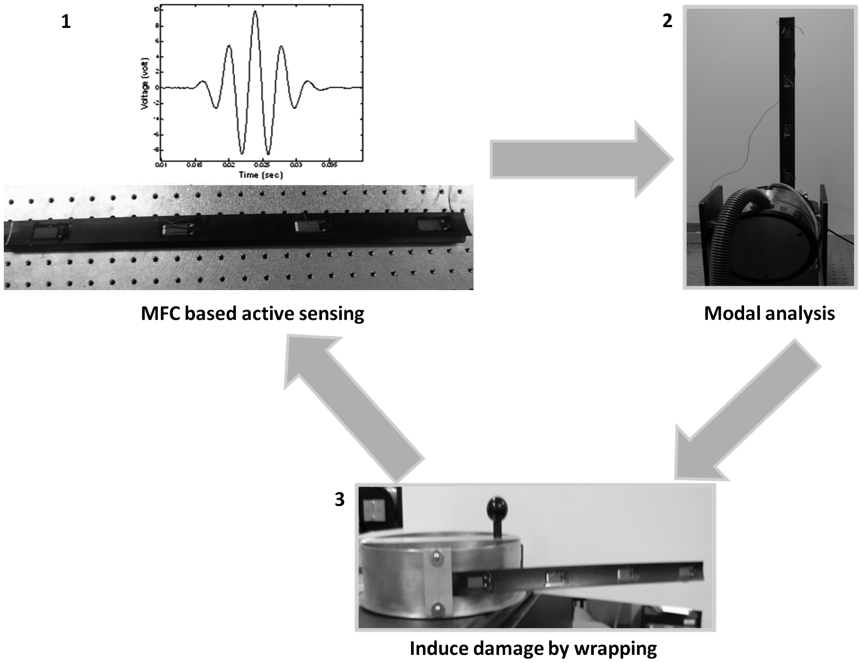

Fig. 6 Experimental test loop for testing deployable boom specimen.

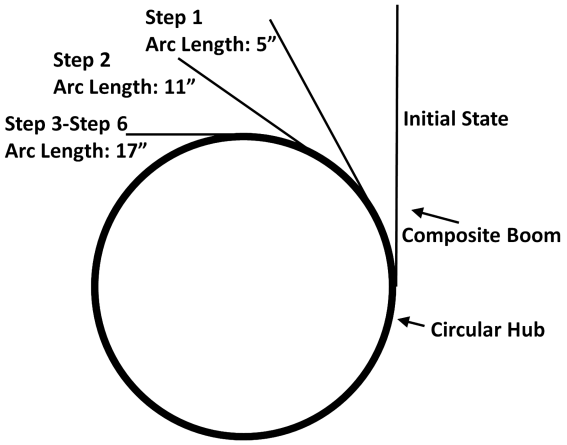

Fig. 7 Six storage states for the composite-boom flattening/wrapping test.

used (arc length of 17 in.) to introduce matrix cracks to the boom structure. After a new storage state was generated, the boom specimen was fully deployed to the original position.

Current nondestructive evaluation techniques, such as flash thermography and ultrasonic scan, can hardly detect matrix cracking in composites. However, matrix cracking and structural stiffness degradation can be detected by the shift of resonant modes using vibration modal analysis. To validate the matrix cracking induced by flattening and wrapping of the boom, the first three resonant modes were measured experimentally through a scanning-head laser vibrometer coupled with a vibration shaker. The experimental setup of vibration modal analysis is shown in Fig. 8. Three steps were used to ensure that the laser points were in the exact locations during each scan. First, the length from the free end of the boom to the custom-made fixture was the same in each scan. Next, the sample was clamped at the same position on the shaker according to the marks drawn on the shaker fixture. Finally, the vibrometer scan head was fixed and the position of the boom on the shaker was adjusted slightly using the reference points so that each scan was started from the same point, as shown in Fig. 8. The shift of first resonant mode can be seen in Fig. 9. The first resonant mode shows the clearest shift after matrix cracks are induced into the sample. After flattening and wrapping the sample five times, the first resonant mode stops decreasing, which means matrix-cracking damage ceases to increase in the composite-boom sample. The equilibrium state of the boom specimen is achieved.

A 48-channel data acquisition system (National Instruments model PXI 1042) was used for active sensing using the MFC transducers. A broadband sweep signal with frequency varying from 10 to 1 kHz was used for active sensing of the MFCs. The excitation signal is shown in Fig. 10a. A representative sensor signal from MFC 4 at the initial state is shown in Fig. 10b. The power spectral density plots of both the input and output signals at the healthy state and six storage states are shown in Fig. 11. With constant input signals, the differences of the power spectral density at different storage states are not clear. The frequency-response method and the ARX model are used for more sensitive structural degradation identification.

IV. Results and Discussion

A. Frequency-Response Method of Input/Output MFC Transducers

The frequency-response method can be used to analyze the input/output relationship and to nonparametrically understand the key aspects of the system before moving to the more complex parametric modeling stages. The information obtained is the basis for identifying parametric transfer-function models. In this paper, a SISO frequency-response method is used to analyze the change at different storage states. The input signals are collected from MFC 1 and output signals are collected from MFC 4. The sensor input/output signals cover the entire damage area and can be used for global damage characterization. The plots for amplitude and phase versus frequency, which can be calculated using Eqs. (1–5), are showed in Fig. 12.

In Eq. (3) the frequency response is determined from the ratio of the cross-correlation spectrum estimate $S_{yx}(j\varpi)$ and autocorrelation spectrum estimate $S_{xx}(j\varpi)$. The amplitude change of the frequency response at a relatively low-frequency range (from 10 to 200 Hz) is mainly caused by the presence of nonlinear properties when matrix cracks are introduced. The understanding of nonlinearity in damaged composite structures helps to choose a proper model for the transfer-function estimation and design the damage index based on the estimated damage index.

The frequency-response method provides the information to select frequency ranges for the input/output pair to include only relevant data. As shown in Fig. 12, the amplitude has a clear response at a low-frequency range from 10 to 200 Hz. The phase also has obvious responses in the same frequency range. This quick analysis helps to choose the frequency range, which provides useful data for the transfer-function estimation.

A key aspect for the frequency-response method is the direct and accurate identification of time delays. The linear relationship between the time delay τ and frequency-response phase shift with frequency ω (rad/s) is expressed as

$$\delta = -\tau\omega \tag{20}$$

where δ is the angle of phase shift at frequency ω. From the frequency-response plot shown in Fig. 12, the phase shift after storage state 2 has a clear change in the frequency range of 10 to

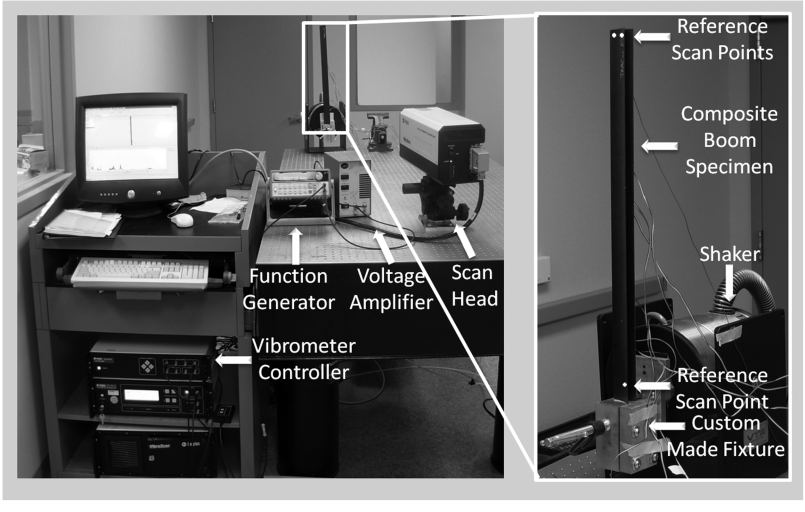

Fig. 8 Experimental setup of vibration modal analysis.

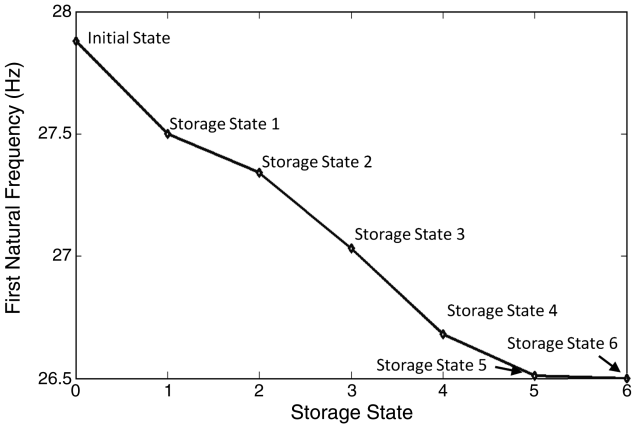

Fig. 9 Resonant mode shift.

200 Hz, which indicates the change of time delay due to induced damage. It can be used as a feature to quickly demonstrate the existence of damage in the composite booms. This also indicates that the time delays are more sensitive in the specific frequency range as more damage is introduced. In the selected sensing frequency range, the velocities of the elastic waves are more sensitive to the change of structural stiffness that is caused by matrix cracking. Since the velocity of elastic wave is a function of the stiffness, the structural stiffness degradation can be estimated using the velocity change of elastic waves in the future research.

B. Transfer-Function Estimation and Order Selection of ARX Model

By carefully choosing the order of the ARX model, SISO transfer functions can be estimated accurately and efficiently. As shown in Eq. (18), the order of the ARX model is the sum of the order of output, n, and the order of input, m. The value of m and n can be different. The criterion of selecting the proper order number is to get the most reasonable estimation with the smallest order number. To find the optimized order number, a set of estimations is needed. Experimental measurements from MFC 1 and MFC 4 at the healthy state are used as the input/output pair for the order analysis. As shown in Fig. 13, the vertical axis, which is called the unexplained output variance, is the ARX model estimation error for the number of orders shown in the horizontal axis. As the order number increases, the estimation error decreases. The order number of the ARX model is the main influence of the estimation error, but each value of m and n is also considered in order to get the minimum order number. Although the estimation accuracy can be improved with a high-order ARX model, the calculation cost increases dramatically. Ideally, by choosing an ARX model with an infinite-order number, the estimation error can be completely removed. However, at the same time, the calculation cost will be infinitely high. After the order number increases up to 40, the slope of estimation error decreases dramatically. In this paper, the order of the ARX model is chosen as 40. In this paper, when the total order of ARX model $(m + n)$ keeps constant and input order m varies from 23 to 33, the estimation error remains approximately constant. Such constancy indicates that total model order $(m + n)$ is the main influence parameter of the model performance. The ARX model has the smallest estimation error when input order m and output order n are chosen as 28 and 12, respectively. An ARX (28,12) is used for the ARX model.

To display the accuracy of the chosen model, one pair of experimental input/output signal collected from MFCs 1 and 4 is used to train and validate the ARX (28,12) model. The first half of the signal in the time domain is used to train the model and the second half of the measured output is compared with the simulated output. The comparison of simulated output signal and experimental output

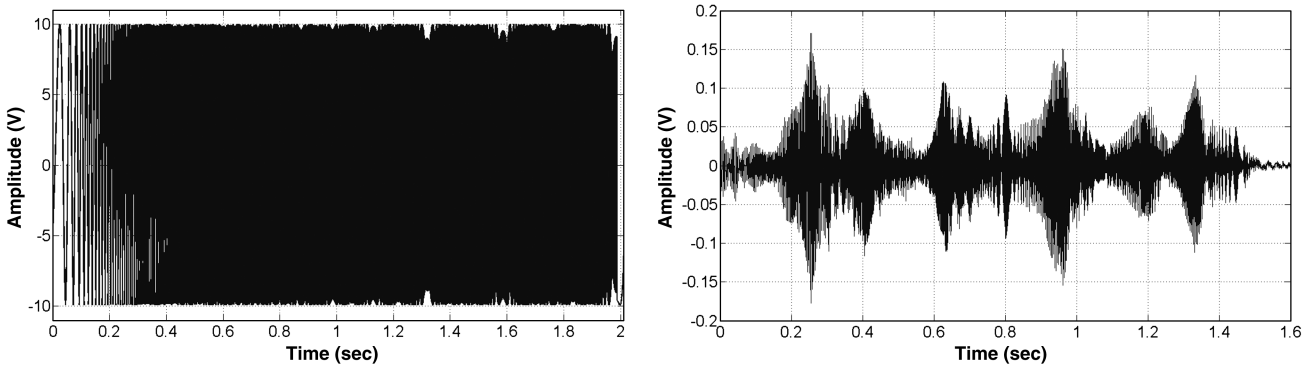

a) b)

Fig. 10 Plots of a) broadband chirp input signal for MFC 1 and b) measured output signal for MFC 4.

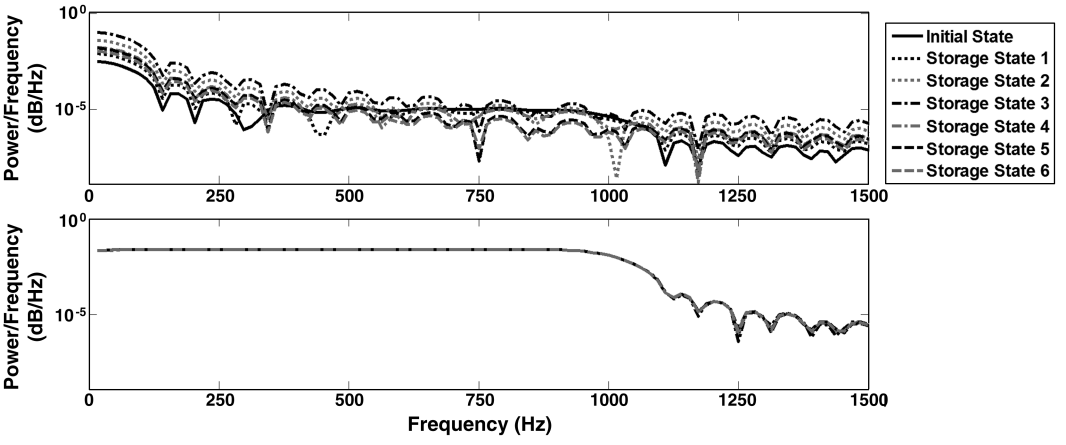

Fig. 11 Power spectral density of input and output MFC 1 and MFC 4 signals at different storage states.

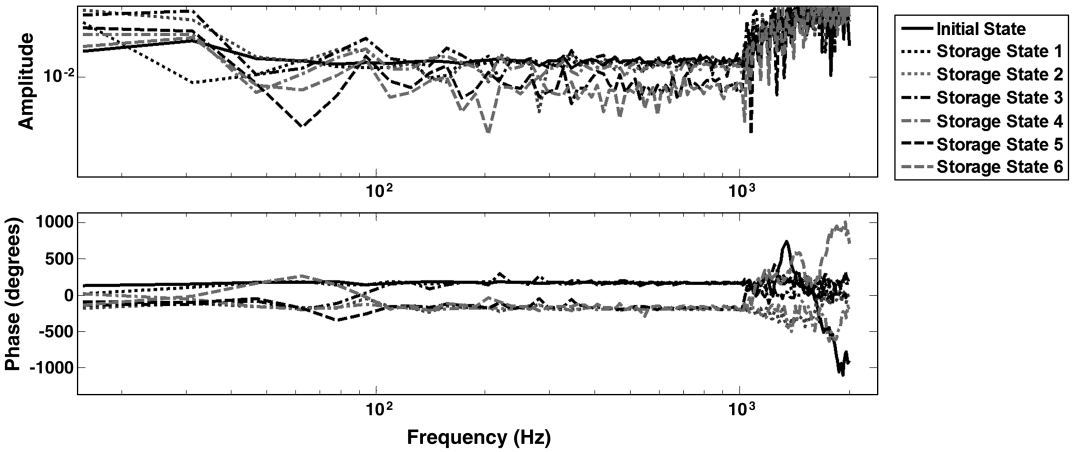

Fig. 12 Frequency response of input/output signal measured from MFCs 1 and 4.

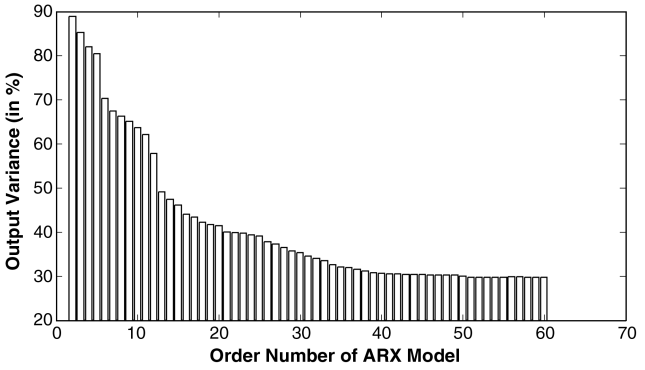

Fig. 13 Estimation error with different order number.

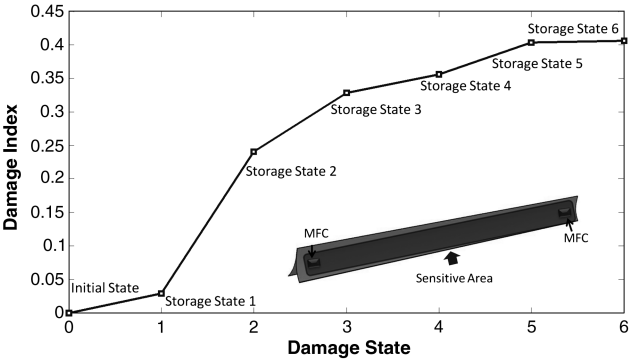

Fig. 15 Global storage-state estimation.

signal can be seen in Fig. 14. The experimental output signal can be accurately simulated by an ARX (28,12) model.

C. Storage-State Identification Using Damage Index

To evaluate the storage state of the entire composite-boom sample subject to flattening and wrapping around the circular hub, both global damage estimation and local damage estimation are carried out. Global damage estimation uses MFCs 1 and 4, which cover the entire boom. The damage index obtained from global damage estimation shows the average damage condition along the entire boom. In Fig. 15, the estimation starts from the healthy state at which the damage index is zero. However, as the flattening and wrapping induces matrix cracking into the boom, the damage index grows gradually. Global structural degradation estimation provides a clear trend of damage growth. Note that the damage caused by matrix cracking is introduced into the boom structure gradually in the first five steps. However, an equilibrium state was detected in step 6. The feature trend obtained from damage-index analysis can be validated by the vibration modal shift analysis, which is shown in Fig. 9.

More damage accumulates in the region between MFCs 1and 2, as this area has been wrapped six times during the experiment. The global structural degradation estimation cannot highlight such local storage states. To concentrate on the hot spot between MFC transducers, local damage estimation analysis is used. The local storage-state estimation for the region between MFCs 1 and 2 is shown in Fig. 16. This region is close to the clamping area of the boom specimen. The damage was induced since step 1. In the first three steps, it is noted that the damage index has a clear increase, which indicates the matrix-cracking propagation during multiple flattening and wrapping procedures. However, the damage index of this region reaches an equilibrium state after step 4. Compared with the global estimation results in Fig. 15, the local storage-state estimation is more sensitive to the matrix-cracking damage. The reason is that the first two storage states contain both healthy and damaged sections in the monitored area. The sensitivity of the

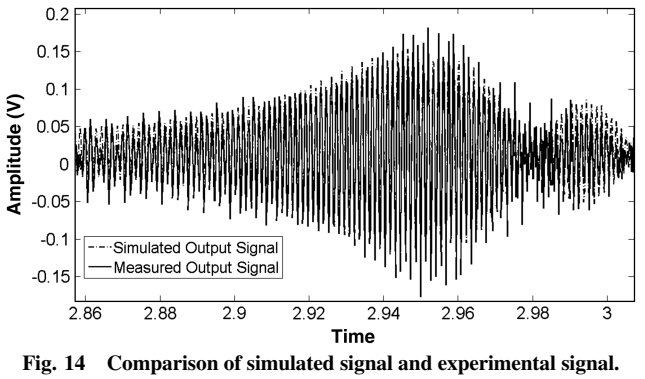

Fig. 14 Comparison of simulated signal and experimental signal.

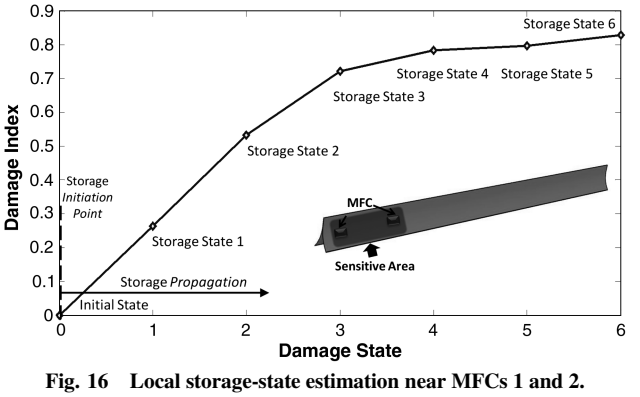

Fig. 16 Local storage-state estimation near MFCs 1 and 2.

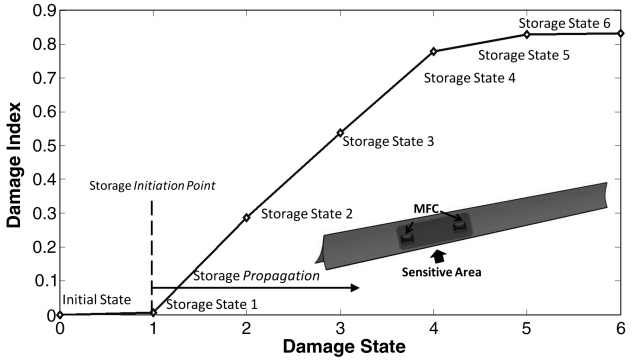

Fig. 17 Local storage-state estimation between MFCs 2 and 3.

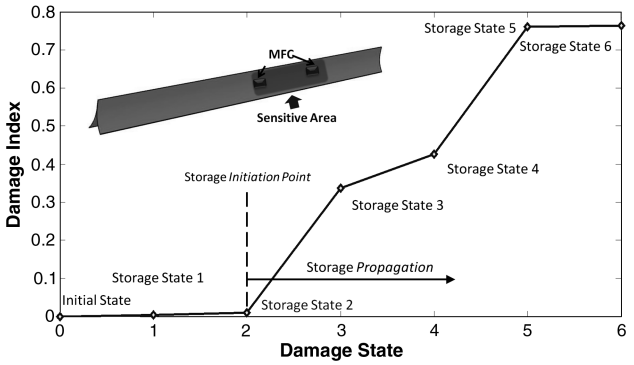

Fig. 18 Local storage-state estimation between MFCs 3 and 4.

damage index decreases as long as the reference becomes larger. Generally speaking, the damage index should provide more sensitivity for local storage-state estimation.

The local storage-state estimation for the section between MFCs 2 and 3 is shown in Fig. 17. As the region was not used in step 1, the damage index keeps constant in this step. Note that the matrix cracking originated in the section between MFCs 2 and 3 in steps 2, 3, and 4. The clear feature trend can be seen in Fig. 17. A similar trend for the damage parameters in the region between MFCs 2 and 3 can be seen as observed from the region between MFCs 1 and 2. An equilibrium state in the local section was achieved after flattening and wrapping the boom specimen three times and the local damage index does not show significant increase in steps 5 and 6. For the region between MFCs 3 and 4, in steps 1 and 2, the local damage index stays near zero, as no severe matrix cracking was introduced, which also indicates a healthy local structural condition, as shown in Fig. 18. The first local matrix cracking was induced in step 3, and the damage-index features keep increasing in steps 3, 4, and 5. However, because the boom specimen reaches an equilibrium condition, the damage index does not increase significantly in step 6. Because all the three local regions reach the equilibrium state in step 6, the global damage index in this step also indicates equilibrium in this step.

V. Conclusions

The system-identification-technique-based structural health monitoring approach is proposed to investigate damage caused by matrix cracking in composite booms subject to flattening and wrapping around a circular hub. Both the frequency-response method and autoregressive with exogenous input model are used to perform single-input/single-output transfer-function estimation and storage-state identification. A flexible macrofiber composite actuator excites the boom specimen and response was captured by three macrofiber composite sensors using low-frequency sweep signals to provide experimental input/output data. The frequency-response method is used to nonparametrically analyze the relationship between input/output sensor signals and select a relevant frequency range. It also provides useful information for the transfer-function analysis using the autoregressive with exogenous input model. The order of the autoregressive with exogenous input model is decided by considering both the estimation accuracy of the model and the calculation cost, and the autoregressive with exogenous input (28,12) model is chosen. The order selection of autoregressive with exogenous input model is validated by comparing the simulated and experimental output signals.

The damage-index estimation, using the residual error of the autoregressive with exogenous input model, provides a clear trend of global damage growth, because the composites will present nonlinear structural properties when matrix cracks are introduced. An equilibrium state for the composite boom was achieved after flattening and wrapping the boom specimens five times. Local storage-state estimation is completed between each macrofiber composite sensor. The newly defined damage index is more sensitive in a localized region, but still provides global state estimation for the entire length of the composite booms. Results show that storage-state estimation using an autoregressive with exogenous input model correlates with the trends seen from first natural-mode shifts using vibration modal analysis techniques. The structural health monitoring system using microfiber composites and autoregressive with exogenous model is a more feasible method of acquiring dynamic characteristics on orbit, as the size, weight, and power requirements are significantly less than with the traditional vibration approach. For future research, the detection of the equilibrium state can be used for the prelaunch quality assurance testing to ensure that a boom structure at equilibrium is inspected before launch. Further research is also needed for qualifying installation methods and hardware for the space environment and analyzing the effect of space conditions on sensing performance.

Acknowledgments

This research is supported by U.S. Air Force Research Laboratory (AFRL), Space Vehicles Directorate, grant FA94530910316. The authors also thank Whitney Reynolds of AFRL for his generous help in this project.

References

[1] Fortescue, P., Stark, J., and Swinerd, G., *Spacecraft Systems Engineering*, Wiley, Chichester, England, U.K., 2003.

[2] Reilly, J., and Terrance, Y., "Autonomous Operations for Responsive Spacecraft," 2006 Responsive Space Conference, AIAA Paper 2006-7001, Reston, VA, April 2006.

[3] Arritt, B., Buckley, S. J., Ganley, J. M., Welsh, J. S., Henderson, B. K., Lyall, M. E., et al., "Development of a Satellite Structural Architecture for Operationally Responsive Space," *Proceedings of SPIE*, Vol. 6930, 2008, Paper 69300I. doi:10.1117/12.776319

[4] Arritt, B., Kumar, A., Buckley, S. J., Hannum, R., Welsh, J. S., Beard, S., et al., "Responsive Satellites and the Need for Structural Health Monitoring," *Proceedings of SPIE*, Vol. 6531, March 2007, Paper 653109. doi:10.1117/12.714424

[5] Harland, D., and Lorenz, R., *Space Systems Failures: Disasters and Rescues of Satellites, Rockets and Space Probes*, Springer–Praxis, New York, 2006.

[6] Price, D. C., Scott, D. A., Edwards, G. C., Batten, A., Farmer, A. J., Hedley, M., et al., "An Integrated Health Monitoring System for an Ageless Aerospace Vehicle," *Proceedings of the 4th International Workshop on Structural Health Monitoring*, Stanford, CA, Sept. 2003, pp. 310–318.

[7] Prosser, W. H., Allison, S. G., Woodard, S. E., Wincheski, R. A., Cooper, E. G., Price, D. C., et al., "Structure Health Monitoring for Future Space Vehicles," *Proceedings of the 2nd Australasian workshop on structural health monitoring*, Monash Univ., Melbourne, Australia, 16–17 Dec. 2004.

[8] Zagrai, A., Doyle, D., Gigineishvili, V., Brown, J., Gardenier, H., and Arritt, B., "Piezoelectric Wafer Active Sensor Structural Health Monitoring of Space Structures," *Journal of Intelligent Material Systems and Structures*, Vol. 21, No. 9, 2010, pp. 921–940. doi:10.1177/1045389X10369850

[9] Liu, Y., Mohanty, S., and Chattopadhyay, A., "Condition Based Structural Health Monitoring and Prognosis of Composite Structures

Under Uniaxial and Biaxial Loading," *Journal of Nondestructive Evaluation*, Vol. 29, No. 3, 2010, pp. 181–188. doi:10.1007/s10921-010-0076-2

[10] Leipold, M., Eiden, M., Garder, C. E., Herbeck, L., Kassing, D., Niederstadt, T., et al., "Solar Sail Technology Development and Demonstration," *Acta Astronautica*, Vol. 52, 2003, pp. 317–326. doi:10.1016/S0094-5765(02)00171-6

[11] Leipold, M., Runge, H., and Sickinger, C., "Large SAR Membrane Antennas with Lightweight Deployable Booms," *28th ESA Antenna Workshop on Space Antenna Systems and Technologies*, ESA, European Space Research and Technology Centre, Noordwijk, The Netherlands, 2005.

[12] D'Amato, A., Arrit, B. J., Banik, J., Ardelean, E., and Bernstein, D., "Structural Health Determination and Model Refinement for a Deployable Composite Boom," 50th AIAA/ASME/ASCE/AHS/ASC Structures, Structural Dynamics, and Materials Conference, AIAA Paper 2009-2373Palm Springs, CA, May 2009.

[13] Park, J., Ha, S., and Chang, F. K., "Monitoring Impact Events Using a System-Identification Method," *AIAA Journal*, Vol. 47, No. 9, Sept. 2009, pp. 2011–2021. doi:10.2514/1.34895

[14] Sohn, H., Farrar, C. R., Hunter, N. F., and Worden, K., "Structural Health Monitoring Using Statistical Pattern Recognition Techniques," *Journal of Dynamic Systems, Measurement, and Control*, Vol. 123, No. 4, Dec. 2001, pp. 706–711. doi:10.1115/1.1410933

[15] Mohanty, S., Chattopadhyay, A., Wei, J., and Pelralta, P., "Unsupervised Time-Series Fatigue Damage State Estimation of Complex Structure Using Ultrasound Based Narrowband and Broadband Active Sensing," *Structural Durability and Health Monitoring*, Vol. 5, No. 3, 2009, pp. 227–250.

[16] Klein, V., and Morelli, E. A., *Aircraft System Identification: Theory and Practice*, AIAA, Reston, VA, 2006.

[17] Yoshida, H., and Kumar, S., "ARX and AFMM Model-Based On-Line Real-Time Data Base Diagnosis of Sudden Fault in AHU of VAV System," *Energy Conversion and Management*, Vol. 40, No. 11, 1999, pp. 1191–1206. doi:10.1016/S0196-8904(99)00022-9

[18] Yang, M., and Makis, V., "ARX Model-Based Gearbox Fault Detection and Localization Under Varying Load Conditions," *Journal of Sound and Vibration*, Vol. 329, No. 24, 2010, pp. 5209–5221. doi:10.1016/j.jsv.2010.07.001

[19] Juang, J.-N., *Applied System Identification*, Prentice–Hall, Upper Saddle River, NJ, 1994.

[20] Polimeno, U., and Meo, M., "Detecting Barely Visible Impact Damage Detection on Aircraft Composites Structures," *Composite Structures*, Vol. 91, No. 4, Dec. 2009, pp. 398–402. doi:10.1016/j.compstruct.2009.04.014

[21] Van Den Abeele1, K. E.-A., Johnson, P. A., and Sutin, A., "Nonlinear Elastic Wave Spectroscopy Techniques to Discern Material Damage, Part i: Nonlinear Wave Modulation Spectroscopy," *Research in Nondestructive Evaluation*, Vol. 12, No. 1, Sept. 2000, pp. 17–30.

[22] Van Den Abeele1, K. E.-A., Carmeliet, J., Ten Cate, J. A., and Johnson, P. A., "Nonlinear Elastic Wave Spectroscopy Techniques to Discern Material Damage, Part II: Single Mode Nonlinear Resonance Acoustic Spectroscopy," *Research in Nondestructive Evaluation*, Vol. 12, No. 1, Sept. 2000, pp. 31–42.

G. Agnes
Associate Editor